Available online at www.sciencedirect.com

SciVerse ScienceDirect

Journal of the European Ceramic Society 32 (2012) 643–647

www.elsevier.com/locate/jeurceramsoc

Mechanical activation of raw materials in the synthesis of Fe_2O_3–$ZrSiO_4$ inclusion pigment

M. Cannio, F. Bondioli *

Dipartimento di Ingegneria dei Materiali e dell'Ambiente, Università degli Studi di Modena e Reggio Emilia, Via Vignolese 905, 41125 Modena, Italy

Received 25 July 2011; received in revised form 22 September 2011; accepted 1 October 2011
Available online 27 October 2011

Abstract

The traditional ceramic industry has recently witnessed increasing interest in the obtainment of inclusion pigments to stabilize at firing temperature and in the action of molten glass unstable chromospheres such as hematite or cadmium sulphoselenide.

This work focuses in the introduction, before the calcination step, of a high energy milling step (mechanosynthesis) to improve the inclusion efficiency of hematite into the zircon matrix by solid state reaction. In particular the synthesis of hematite–zircon inclusion pigment was optimized through an accurate control of the raw material milling time and calcination temperature. The mechanical activation modifies the conditions in which chemical reactions usually take place changing the reactivity of as-milled solids by increase of reaction rates and lowering the reaction temperatures of ground powders.

Keywords: A. Powders–solid state reaction; A. Calcination; C. Colour; D. Traditional ceramic; Pigment

1. Introduction

Inorganic natural and synthetic pigments produced and marketed as fine powders are an integral part of many decorative and protective coatings and are used for the mass colouration of many materials, including glazes, ceramic bodies and porcelain enamels. In all these applications, pigments are dispersed (they do not dissolve) in the media, to form a heterogeneous mixture. Briefly, powders used to colour ceramics must show thermal and chemical stability at high temperatures and must be inert to the action of molten glass (frits or sintering aids).[1] These characteristics limit ceramic pigments to a very small number of refractory systems, which are fully reacted and relatively inert to the matrix in which they are dispersed.[2–7] In recent years, there has been a developing interest toward inclusion pigments,[1,8–12] which make usable colouring substances tolerant of the industrial thermal and chemical conditions by occluding them in a stable glassy or crystalline matrix (heteromorphic pigments). The inclusion or encapsulation of reactive, coloured or toxic crystals inside stable crystalline or amorphous uncoloured matrixes provides an efficient chromophore protection.

Early works[13] described the preparation of red and orange zircon pigments by inclusion of inorganic compounds (i.e. $Cd(S_xSe_{1-x})$) into the zircon network to obtain pigments with sufficient chemical and thermal stability at firing temperatures. According to the "inclusion pigments" denomination proposed by V.L. Lavilla and J.M. Rincon,[14] this new family of pigments present the following characteristics:

(a) they are composed by two or more different insoluble crystalline structures;
(b) their behaviour in the presence of glazes is like a unique chromatic unit from a pigmentation point of view. The colour is not developed by introduction of coloured ions into matrix lattices or by the formation of solid solutions, but by the inclusion of small coloured crystals into the matrix during the sintering process.

Among the systems studied for such use, hematite included in zircon (DCMA 14-44-5),[15] also known as "coral pink" pigment, is one of the zircon-based pigments, along with vanadium zircon blue ($(V,Zr)SiO_4$) and praseodymium zircon yellow ($(Pr,Zr)SiO_4$), that represent a market leader in high-temperature

* Corresponding author. Tel.: +39 059 2056242; fax: +39 059 2056243.
E-mail address: federica.bondioli@unimore.it (F. Bondioli).

0955-2219/$ – see front matter © 2011 Elsevier Ltd. All rights reserved.
doi:10.1016/j.jeurceramsoc.2011.10.008

applications for the whitewares industry. The traditional synthesis of the "hematite included in zircon/or coral pink" pigment consists in the mixing of an iron precursor (generally Fe_2O_3, $FeSO_4$, or FeO(OH)) with zirconia, silica and several mineralizers (mainly alkaline or alkaline earth halides) and the firing of the obtained mixture at temperatures such as 900 °C.[16] Zircon formation and hematite coarsening have to occur simultaneously to guarantee efficient hematite occlusion and a high colour yield.[11] The control of these two steps is fundamental for appropriately growing chromophore particles in the same range of temperatures as that for zircon formation, so that the chromophore particles can be trapped by the matrix particles during sintering. The choice of an appropriate mineralizer becomes particularly important.

In this work, a high energy milling step (mechanosynthesis) was applied to the raw materials before the calcination step to improve the inclusion efficiency of hematite into the zircon matrix by solid state reaction. The intrinsic advantage of mechanosynthesis is that the solid-state reaction is activated by mechanical energy instead of temperature. High-energy ball-milling enables to modify the conditions in which chemical reactions usually take place changing the reactivity of as-milled solids (mechanical activation[17]) by increase of reaction rates, lowering the reaction temperatures of ground powders and inducing chemical reactions during milling (mechanochemistry[18–20]). Mechanical activation has been used in the synthesis of other ceramic pigments such as nano-crystalline ZnO–CoO[21] or alumina-based pigments,[22,23] however, as far as we are concerned, the effect of mechanical activation on the synthesis of hematite–zircon red ceramic pigment has still not been investigated.

In particular, the effect of specific process variables such as milling time (at a fixed milling rate), and calcination temperature was investigated in order to optimize the inclusion of hematite in the zircon matrix. Colour tests were performed on a porcelainized stoneware ceramic glaze loaded with 4 wt% of as-synthesized pigments and fired in a semi-industrial kilns to verify the applicability of the investigated pigments into industrial glazes.

2. Experimental procedure

2.1. Powder synthesis

Industrial-quality monoclinic ZrO_2, SiO_2 (α-quartz), and α-Fe_2O_3, as well as mineralizers (KCl, 2 wt%, and KNO_3, 2 wt%), were selected as raw materials for the pigment preparation. SiO_2 and ZrO_2 were mixed in order to obtain the stoichiometric composition of zircon with a 15 wt% of α-Fe_2O_3. All the raw materials employed in this investigation were used in as-received state without any purification or grinding to reproduce the industrial process. The powders were charged in a cylindrical agate vial of 40 mm in diameter together with agate balls of 12 mm diameter. All the experiments were performed in a Fritsch Pulverisette 7 planetary ball mill using a rotation speed of 200 rpm keeping constant ball-to-powder weight ratio at 20:1. Milling was interrupted every hour for 30 min to prevent significant increases in powder temperature. The milling time were changed in the 15–480 min range to study the effect of mechanosynthesis on both pigment grain size distribution and degree of inclusion. Hence, the obtained mixtures were calcined in closed porcelain crucibles with heating rates of 10 °C/min at different temperatures (1000–1200 °C) for 2 h of soaking time and then wet milled. Finally, the obtained powders were tested as pigments for glaze colouring. A porcelainized stoneware ceramic glaze was used for pigment application. The pigments, added to the composition at 4 wt%, were wet mixed with the ceramic frit for 30 min in a blender-mixer and then deposited by a roller blade in a ceramic body. The obtained tiles were fired in an industrial high-speed roller kiln using a typical industrial cycle of ∼35 min with a maximum temperature of 1140 °C.

2.2. Powder characterization

Thermal behaviour of the mechanically activated mixtures was studied in air using a simultaneous thermogravimetric and differential thermal analyzer (TG-DTA, mod. 409, Netzsch). About 30 mg of powdered samplewith grain size lower than 25 μm in grain size were subjected to a thermal treatment from 20 to 1400 °C at a heating rate of 10 °C/min.

X-ray diffraction measurements (XRD) were carried out using a conventional Bragg–Brentano diffractometer (PW 3710, Philips Research Laboratories) with Ni-filtered CuKα radiation to determine the crystalline phases present on the samples. The patterns were recorded on grounded samples (<25 μm in size) in the 20–80° 2θ range at room temperature, with a scanning rate of 0.005°/s and a step size of 0.02°. The morphology and microstructure of the samples were examined by scanning electron microscopy (SEM) (XL40, Philips Research Laboratories) equipped with an energy dispersion spectroscopy (EDS) equipment (EDAX, Philips Research Laboratories).

The colour measurements were performed by UV–Vis spectroscopy (model Lambda 19, Perkin Elmer) using the CIELab method in order to obtain L^*, a^* and b^* values. This method, which is the standard analysis in the ceramic industry, allows to determine the whiteness and colour degree of tiles by measuring the three parameters L^* (brightness), from absolute white $L^* = 100$ to absolute black $L^* = 0$, a^* (red–green) and b^* (yellow–blue) elaborated from the visible spectra.

3. Results and discussion

3.1. Milling time optimization

In Fig. 1a the DTA curve of the raw material mixture after 60 min of mechanical synthesis is reported as representative. The curve presents an endothermic peak at around 100 °C due to humidity elimination and an exothermal peak at around 1100 °C due to $ZrSiO_4$ formation. From the overlapped view of the DTA curves of the powders milled at different times reported in Fig. 1b), it is evident the shift of the zircon formation peak to lower temperatures as the milling time is increased. This behaviour clearly shows that the mechanical synthesis changed

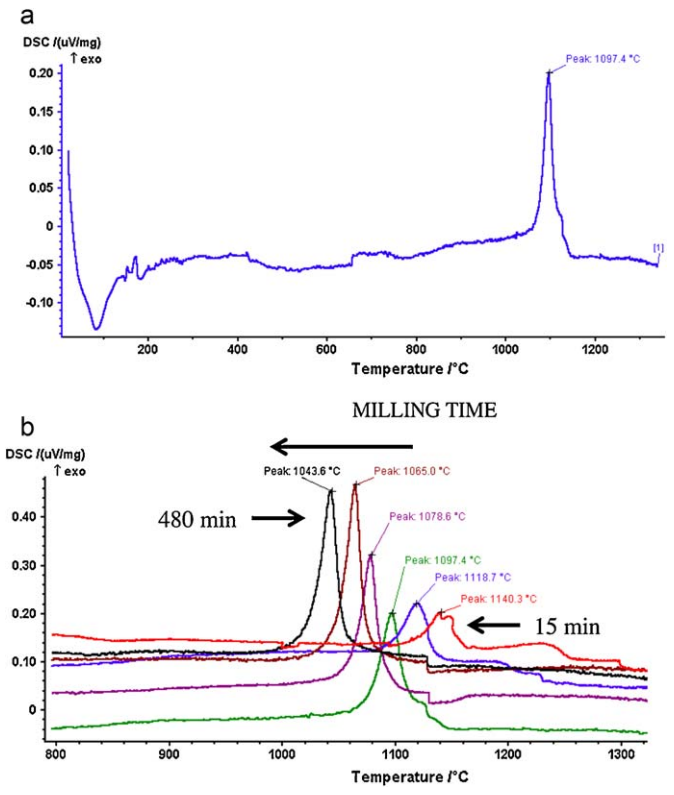

Fig. 1. DTA curve of the sample milled for 60 min (a) and overlapped view of the DTA curves of powders milled in the range 15–480 min (b).

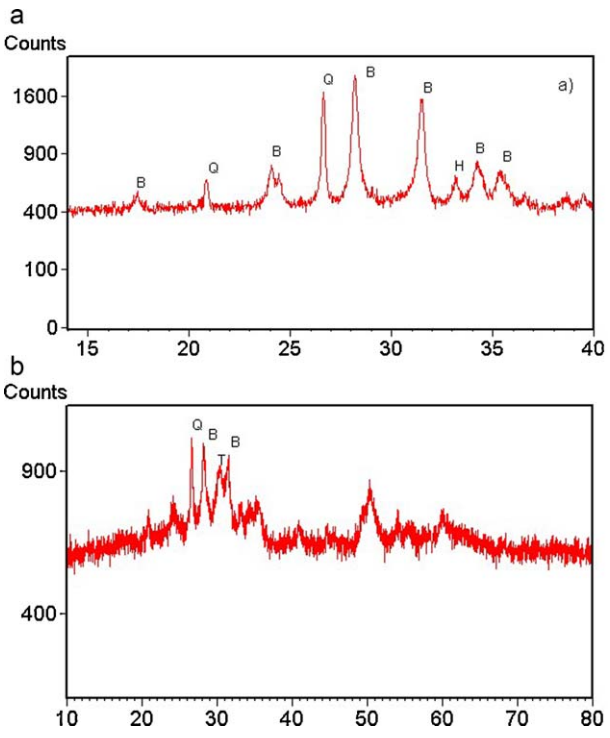

Fig. 2. XRD pattern of the raw mixture milled for 15 min (a) and 240 min (b) of mechanical synthesis. B = m-ZrO_2; Q = quartz; H = Fe_2O_3; T = t-ZrO_2.

the reactivity of as-milled solids having an activation effect on the zircon structure crystallization.

In Fig. 2 the XRD patterns of the raw milled samples are reported. In particular, the pattern of the powder milled for 15 min (Fig. 2a) shows the presence of baddeleyite (ICDD #24-1165), quartz (ICDD #33-1161) and α-hematite (ICDD #33-664). After 240 min of milling (Fig. 2b), the sharp crystalline lines of the starting powders disappear and a relative broad diffuse pattern shows up. This amorphization is a clear indication that the crystal structures of the starting materials were modified by high energy ball milling. Moreover, starting from the powder milled for 240 min, a series of new lines appear attributable to the t-ZrO_2 phase (ICDD #17-0923), while those of m-ZrO_2 remain. Peak position indicated that this phase could be a t-ZrO_2 solid solution being the peaks slightly at higher diffraction angles if compared with the characteristic ones. In particular, taking into account the ionic radii (Fe^{3+} = 63 pm; Zr^{4+} = 79 pm) a tetragonal phase stabilization due to iron could be hypothesized.

The mechanically activated powders were calcined at 1100 °C. Independently on the milling time, the XRD patterns (Fig. 3) underlined the presence of zircon (ICDD #6-266), m-ZrO_2 and α-hematite. In particular, the figure shows that the intensity of monoclinic zirconia peaks decreases as the milling time is increased in agreement with the higher reactivity of powders milled for longer time. In Table 1, the CIElab values of the calcined powders are reported. In particular, the a^* parameter, that indicates the predominance of the red colour (positive values) on the green colour (negative values), is for this pigment the most representative value. The table shows that the a^* parameter increases as the milling time is increased underlining that the red colour of fired powders is mainly dominated by the amount of size of free hematite particles. This result can be commented taking into account several factors that are crucial for the inclusion process. In particular it can be hypothesized that, as the milling time increases, the inclusion process is less efficient due to both the formation of the tetragonal solid solution and the enhancement of zircon crystallization rate. Moreover, the inclusion process is also surely less efficient due to the smaller size of free hematite particles during the zircon crystallization and sintering as evidenced by the increase of specific surface area values (Table 3) as the milling time is increased.

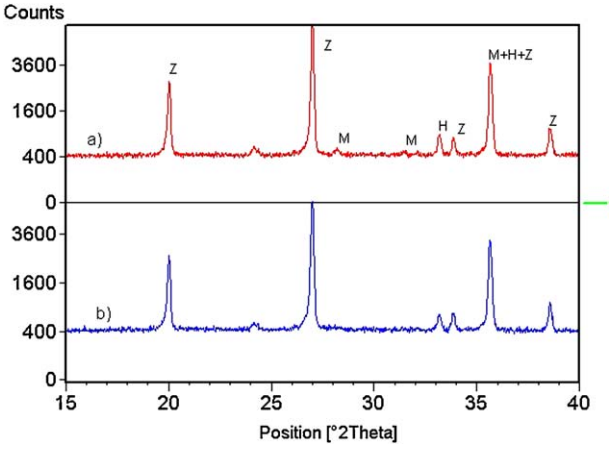

Fig. 3. XRD pattern of the pigments milled for 15 (a) and 240 min (b) and calcined at 1100 °C. Z = $ZrSiO_4$; B = m-ZrO_2; H = Fe_2O_3.

Table 1
CIELab values of samples milled for different time and calcined at 1100 °C.

Milling time (min)	L^*	a^*	b^*
0	46.88	10.33	4.91
15	43.80	11.35	6.41
30	43.99	11.68	6.79
120	43.80	11.91	7.04
240	44.26	13.34	7.90
480	43.85	13.92	8.88

Table 2
CIELab values of glazed obtained with pigment milled for different time (calcination temperature 1100 °C).

Milling time (min)	L^*	a^*	b^*
0	58.00	18.73	18.92
15	57.19	29.37	28.63
30	60.49	25.35	25.81
60	56.48	26.67	28.34
120	60.99	27.43	32.16
240	67.71	26.08	35.32
480	69.28	20.53	33.38

The CIELab values of the coloured glazes, reported in Table 2, indicate that, independently on the milling time, the mechanically activated powders have always a higher value of the a^* parameter. Moreover, Table 2 shows that the best colour, characterized by the highest a^* values, can be obtained with a milling time of 15 min. This result could be explained considering that for shorter milling time, the efficacy of the inclusion process is higher. In fact above the optimal milling time, hematite particles would be less efficiently included (due to their smaller size and to the faster rate of zircon crystallization) and thus less efficiently protected by zircon grains against the action of molten glass during the enamel firing.

In conclusion, the analysis of the obtained results suggests that the best milling time is 15 min.

3.2. Calcination temperature optimization

The XRD patterns of the obtained pigments (Fig. 4) show that, independently on the calcination temperature, the crystallographic phases present in the samples are zircon, m-ZrO_2 and α-hematite. In particular, analysing the peak intensity, it is evident that as the temperature increases the peak intensity of monoclinic zirconia decreases due to the higher reactivity. The

Table 3
Specific surface area (SSA) values of the calcined pigments as a function of milling time.

Milling time (min)	Temperature (°C)	SSA (m^2/g)
480	1100	8.23
15	1100	0.75
15	1000	0.62
15	1050	0.74
15	1150	0.85
15	1200	0.75

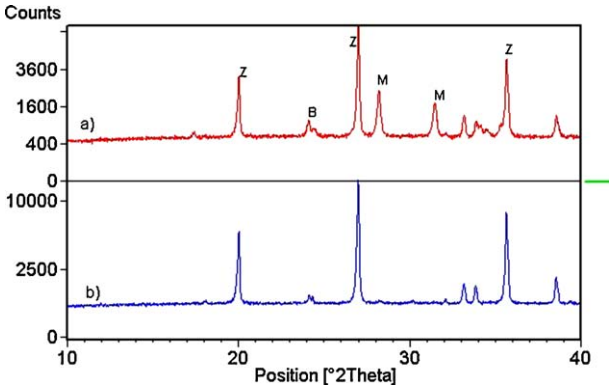

Fig. 4. XRD pattern of the mixture milled for 15 min and calcined at 1000 (a), and 1200 °C (b). Z = $ZrSiO_4$; M = m-ZrO_2; H = Fe_2O_3.

Table 4
CIELab values of pigment calcined at different temperature(milling time 15 min).

Calcination temperature (°C)	L^*	a^*	b^*
1000	42.89	14.12	8.15
1050	43.18	13.78	7.34
1100	43.80	11.35	6.41
1150	44.84	10.85	6.83
1200	45.28	10.42	5.65

SSA values (Table 3) of the pigments obtained at different calcination temperatures do not show any important differences as confirmed by SEM analysis (Fig. 5). Fig. 5 also puts in evidence that the size of the pigment particles is in the 0.5–2 μm range.

In Tables 4 and 5 the colour of pigments and glazes are reported as a function of calcination temperature at a constant milling time of 15 min. In particular the a^* parameter of glazes increases as the temperature of pigment calcination is increased with an opposite behaviour with respect of the pigment colour. It could be hypothesized that for the pigments, the calcination temperature directly influences the inclusion efficiency. In fact, although the red colour of the fired pigments decreases with the increase of firing temperature (probably due to the higher particle size of free hematite particles), the hematite particles are more efficiently included as a result of the improved sintering leading to a higher resistance towards the action of the molten glasses and thus to a higher chromophore efficiency. As a consequence, the a^* parameter of the glazes increases as the pigment calcination temperature is increased. Table 5 puts in evidence that from 1100 °C the values are similar indicating that 1100 °C

Table 5
CIELab values of glazes obtained with pigment calcined at different temperature (15 min milling time).

Calcination temperature (°C)	L^*	a^*	b^*
1000	61.46	15.36	22.45
1050	58.87	24.76	28.54
1100	57.19	29.37	28.63
1150	53.46	28.95	28.45
1200	51.82	29.56	28.93

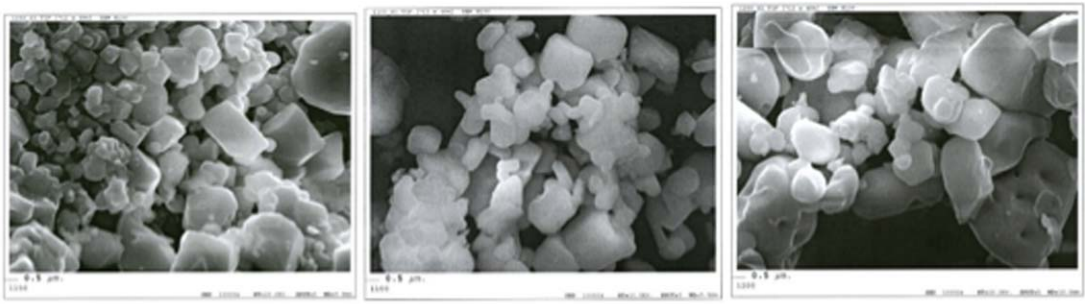

Fig. 5. SEM images of the pigment calcined at 1100 (a), 1150 (b) and 1200 °C (c). Milling time 15 min.

could be considered the optimal temperature to obtain a good inclusion efficiency.

4. Conclusion

The obtained results suggest that the mechanosynthesis is an efficient method to activate the raw materials for the synthesis of the inclusion pigment Fe_2O_3–$ZrSiO_4$.

In particular, the mechanical activation increases the reactivity of the mixture decreasing, as the milling time is increased, the characteristic temperature of zircon formation. However, the obtained results underline the extreme importance of the milling time optimization. The optimal milling time condition is 15 min since a further increase of milling time results in the stabilization of tetragonal zirconia by iron in the raw mixture and at the same time in the lowering of the grain size of free hematite, which appears to be detrimental for the efficacy of hematite inclusion after the firing treatment. The effect of calcination temperature is also of crucial importance: the increase of firing temperature appears to result in more efficiently included hematite particles within the zircon grains as underlined by the higher red hue developed in the ceramic glasses, indicating 1100 °C as the optimal firing temperature.

References

1. Vicent JB, Llusar M, Badenes J, Tena MA, Vicente M, Monros G. Occlusion of chromophore oxides by sol–gel methods: application to the synthesis of hematite–silica red pigments. *Bol Soc Esp Ceram Vidrio* 2000;**39**(1):83–93.
2. Procyk B, Kucharski J, Stoch L. Ecological red pigments based on copper glass. *Ind Ceram* 1997;**926**:342–4.
3. Bondioli F, Manfredini T. The search for new red pigments. *Am Ceram Soc Bull* 2000;**79**(2):68–70.
4. Jansen M, Letschert P. Inorganic yellow–red pigments without toxic metals. *Nature* 2000;**404**(6781):980–2.
5. Aruna ST, Ghosh S, Patil KC. Combustion synthesis and properties of $Ce_{1-x}Pr_x\ O_{2-\delta}$ red ceramic pigments. *Int J Inorg Mater* 2001;**3**(4–5):387–92.
6. Baldi G, Dolen N. Synthesis of a new class of red pigments based on perovskite type lattice $A_xB_{(2-x-y)}CrYO_3$ with $x = 0.9 - 1.1$, $y = 0.05 - 0.12$ A = Y, Lanthanides, B = Al for use in body stain and high temperature glazes. Effect of Cr^{+++} and metal A on the colour of ceramic pigment. *Mater Eng* 1999;**10**(2):151–64.
7. Olazcuaga R, Le Flem G, Alarcon J. Introduction of Tb^{4+} into CeO_2 to obtain stable red pigments at high temperatures. *Bol Soc Esp Ceram Vidrio* 1993;**32**(5):307–10.
8. Bondioli F, Ferrari AM, Leonelli C, Manfredini T. Synthesis of Fe_2O_3/Silica red inorganic inclusion pigments for ceramic application. *Mat Res Bull* 1998;**33**(5):723–9.
9. Llusar M, Badenes JA, Calbo J, Tena MA, Monros G. Environmental and colour optimisation of mineraliser addition in synthesis of iron zircon ceramic pigment. *Br Ceram Trans* 2000;**99**(1):14–22.
10. Bondioli F, Manfredini T, Siligardi C, Ferrari AM. New glass–ceramic inclusion pigment. *J Am Ceram Soc* 2005;**88**(4):1070–1.
11. Garcia A, Llusar M, Badenes J, Tena MA, Monros G. Encapsulation of hematite in zircon by microemulsion and sol–gel methods. *J Sol–Gel Sci Technol* 2003;**27**:267–75.
12. Llusar M, Royo V, Badenas JA, Tena MA, Monros G. Nanocomposite Fe_2O_3–SiO_2 inclusion pigments from post-functionalized mesoporous silicas. *J Eur Ceram Soc* 2009;**29**:3319–32.
13. Lambies Lavilla V. Considerations on a zircon–cadmium sulfoselenide pigment. *Ceram Inform* 1978;**13**:405–10.
14. Lambies Lavilla V, Rincon Lopez JM. Study of the mechanism of formation of zircon–cadmium sulphoselenide pigment. *J Br Ceram Soc* 1981;**80**:105–8.
15. Dry Colors Manufacturers Association (DCMA). *Classification and chemical description of the mixed metal inorganic coloured pigments*. 2nd ed. Washington, DC, USA: DCMA; 1982.
16. Berry FJ, Eadon D, Holloway J, Smart LE. Iron-doped zircon: the mechanism of formation. *J Mater Sci* 1999;**34**:3631–8.
17. Temuujin J, Okada K, Mac Kenzie KJD. Formation of mullite from mechanochemically activated oxides and hydroxides. *J Euro Ceram Soc* 1998;**18**:831–5.
18. Corrias A, Paschina G, Sirigu P. Ni–silica and Cu–silica nanocomposites prepared by ball milling. *J Non-Cryst Solids* 1998;**232–234**: 358–63.
19. Matteazzi P, Le Caër G. Synthesis of nanocrystalline alumina-metal composites by room temperature ball-milling of metal oxides and aluminum. *J Am Ceram Soc* 1992;**75**(10):2749–55.
20. Hue J, Wan D, Lee See-Ee, Wang J. Mechanochemical synthesis of lead zirconate titanate from mixed oxides. *J Am Ceram Soc* 1999;**82**(7): 1687–92.
21. Rasouli S, Jebeli-Moeen S, Arabi AM. Synthesis of wurtzite nanocrystalline ZnO–CoO pigment by high energy milling. *Prog Color Colorants Coat* 2009;**2**:45–51.
22. Ricceri R, Ardizzone S, Baldi G, Matteazzi P. Ceramic pigments obtained by sol–gel techniques and by mechanochemical insertion of color centers in Al_2O_3 host matrix. *J Eur Ceram Soc* 2002;**22**: 629–37.
23. Costa AL, Cruciani G, Dondi M, Matteucci F. New outlooks on ceramic pigments. *Ind Ceram* 2003;**23**:1–11.